

Free axial vibration analysis of axially functionally graded thick nanorods using nonlocal Bishop's theory

Reza Nazemnezhad ^{*1} and Kamran Kamali ^{2,3a}

¹ School of Engineering, Damghan University, Damghan, Iran

² Impact Research Laboratory, Department of Mechanical Engineering, Iran University of Science and Technology, Tehran, Iran

³ Department of Design, Fateh Sanat Kimia Company, Great Industrial Zone, Shiraz, Iran

(Received November 16, 2017, Revised May 17, 2018, Accepted July 6, 2018)

Abstract. Free axial vibration of axially functionally graded (AFG) nanorods is studied by focusing on the inertia of lateral motions and shear stiffness effects. To this end, Bishop's theory considering the inertia of the lateral motions and shear stiffness effects and the nonlocal theory considering the small scale effect are used. The material properties are assumed to change continuously through the length of the AFG nanorod according to a power-law distribution. Then, nonlocal governing equation of motion and boundary conditions are derived by implementing the Hamilton's principle. The governing equation is solved using the harmonic differential quadrature method (HDQM). After that, the first five axial natural frequencies of the AFG nanorod with clamped-clamped end condition are obtained. In the next step, effects of various parameters like the length of the AFG nanorod, the diameter of the AFG nanorod, material properties, and the nonlocal parameter value on natural frequencies are investigated. Results of the present study can be useful in more accurate design of nano-electro-mechanical systems in which nanotubes are used.

Keywords: nonlocal theory; Bishop's theory; axially functionally graded nanorod; axial vibration; harmonic differential quadrature method

1. Introduction

It is clear that in each field of science and technology using an element in design of a mechanical system requires identification of the accurate mechanical behaviors of that element. One of these science and technology fields which it attracts attention of a lot of scientists and researchers is nanotechnology field. In nanotechnology field there are several methods for investigation of mechanical behaviors of systems. Between these methods, the use of theoretical ones and mathematical modelling are more common because they are low cost and available to everyone. Like macro domain which mathematical models of plate, shell, beam, rod and bar are used for analysis of macro elements, in nano domain mathematical models of nanoplate, nanoshell, nanobeam, nanorod and nanobar are implemented.

Between the mathematical models of mechanical elements, the nanorod model is used for modelling of elements that their axial mechanical behavior like free axial vibration is desired. These elements can be single- or multi-walled nanotubes or nanorods made of aluminum or silicon. In this regard, Aydogdu (2009) investigated the axial vibration of nanorods modeled based on the simplest rod theory by using the nonlocal elasticity theory. In another

similar work, Kiani (2010) considered the small scale effect on free longitudinal vibration of nanowires with linearly varied radii. This work also used the simplest rod theory for modelling of the tapered nanorods. A similar investigation on the longitudinal vibration of double-nanorod-systems was also found by Murmu and Adhikari (2010). In a different work, the surface energy effects on the longitudinal and transverse wave propagation of nanotubes embedded in elastic medium are considered (Assadi and Farshi 2011). The effect of nonlocality is also considered on the longitudinal vibration of nanobeams with crack (Hsu *et al.* 2011). This effect is also studied on the analysis of the axial wave propagation of coupled nanorod systems (Narendar and Gopalakrishnan 2011). Goushegir and Faroughi (2016) studied the small scale effect on the axial vibration of non-uniform nanorods using boundary characteristic orthogonal polynomials. The simple rod model is also used for modelling and analysis of mechanical behaviors of nanorods made of functionally graded materials. In another work, the free longitudinal vibration of axially functionally graded tapered nanorods with variable cross-section was studied based on the nonlocal elasticity theory (Şimşek 2012). In the work, elasticity modulus and mass density of the nanorod vary continuously in the axial direction of the nanorod according to a power-law form. By using the strain gradient theory, the longitudinal vibration of nanorods made of functionally graded materials is analyzed (Akgöz and Civalek 2013). The rod model was also utilized by Aydogdu (2014) for modelling of axial vibration of double-walled carbon nanotubes. In this study, the Van der

*Corresponding author, Ph.D., Assistant Professor,
E-mail: rnazemnezhad@du.ac.ir

^aM.Sc. of Mechanical Engineering

Waals forces were considered in the axial direction and the small scale effect was investigated on natural axial frequencies of nanotubes. Karličić *et al.* (2015) investigated the nonlocal longitudinal vibration of viscoelastic coupled double-nanorod systems. Besides these studies, there are some references (Nguyen *et al.* 2014, Rahmani *et al.* 2017, Simsek, 2011, Adhikari *et al.* 2013, 2014, Akgöz and Civalek 2011, 2017, Allahkarami *et al.* 2017, Amar *et al.* 2018, Belkhorissat, Houari, & Tounsi, Adda, & Mahmoud, (2015), Bounouara *et al.* 2016, Faroughi and Shaat 2017, Faroughi *et al.* 2017, Goushegir and Faroughi 2017) in which the bending, buckling, and vibration of nonlocal beams and plates are considered.

The above literature survey shows that the main goal of published works is considering the small scale effect on axial vibration of homogenous and functionally graded nanorods and nanotubes with constant or variable cross section. To this end, nanorods and nanotubes are modeled based on the simplest rod theory in which the inertia of the lateral motions and shear stiffness are neglected. While this theory cannot be a good choice for considering axial mechanical behavior of thick nanorods. Because the inertia of lateral motions and shear stiffness effects become noticeable in thick nanorods. There are only two studies using the Bishop's theory for considering the behavior of thick nanorods (Güven 2014, Li *et al.* 2017), "These studies have considered a homogeneous material for nanorods.

Since there is no work to study the influences of the shear stiffness and the inertia of the lateral motions on the free axial vibration of nanorods with functionally graded materials, the present work aims to cover this issue. To this end, nanorods with axially functionally graded (AFG) material and constant cross section are considered. Then, governing equation of motion and boundary conditions are derived by using the Hamilton's principle. In the next step, the differential model of the nonlocal elasticity theory is implemented to obtain the nonlocal governing equation of motion and boundary conditions. To solve the governing equation of motion, the harmonic differential quadrature method is utilized and the axial natural frequencies are obtained for clamped-clamped end condition. Finally, effects of various parameters like nonlocal parameter, shear stiffness and inertia of lateral motions, nanorod dimensions, frequency number, boundary condition type, and gradient index number on natural axial frequencies of AFG nanorods are investigated in details.

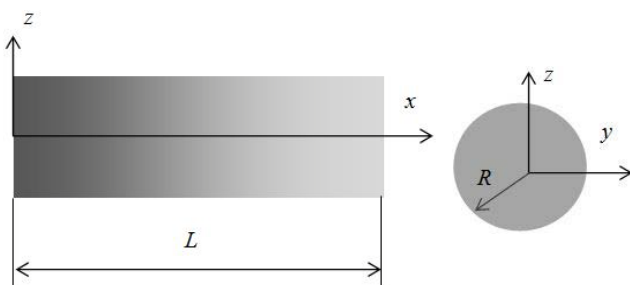


Fig. 1 Geometry of an AFG nanorod

2. Problem formulation

Consider an AFG nanorod with length L ($0 \leq x \leq L$) and circular cross section A with radius R . The AFG nanorod is generally composed of two different materials at the left and the right ends (as shown in Fig. 1).

Poisson's ratio is assumed to be constant, i.e., $\nu = 0.3$, whereas bulk elastic modulus $E(x)$, shear modulus $G(x)$, and mass density $\rho(x)$ are assumed to vary in the axial direction according to the power law distribution

$$\begin{aligned} E(x) &= (E_L - E_R) \left(1 - \frac{x}{L}\right)^m + E_R \\ G(x) &= (G_L - G_R) \left(1 - \frac{x}{L}\right)^m + G_R \\ \rho(x) &= (\rho_L - \rho_R) \left(1 - \frac{x}{L}\right)^m + \rho_R \end{aligned} \quad (1)$$

where the subscripts L and R denote the left ($x = 0$) and right ($x = L$) ends of nanorod, respectively, and a gradient index m determines the variation profile of material properties across the AFG nanorod length. Upon the Bishop rod model, considering the effects of the inertia of the lateral motions and the shear stiffness, the displacement field at any point of the nanorod can be written as

$$u = u(x, t); \quad v = -\nu y \frac{\partial u}{\partial x}; \quad w = -\nu z \frac{\partial u}{\partial x}; \quad (2)$$

where u , v and w are the displacement components of the nanorod along x , y and z coordinates, respectively. According to Eq. (2), the non-zero strain components in the cross section can be obtained as

$$\begin{aligned} \varepsilon_{xx} &= \frac{\partial u}{\partial x}; \\ \varepsilon_{yy} &= \frac{\partial v}{\partial y} = -\nu \frac{\partial u}{\partial x}; \\ \varepsilon_{zz} &= \frac{\partial w}{\partial z} = -\nu \frac{\partial u}{\partial x}; \\ \varepsilon_{yz} &= \left(\frac{\partial v}{\partial z} + \frac{\partial w}{\partial y}\right) = 0; \\ \varepsilon_{xy} &= \left(\frac{\partial u}{\partial y} + \frac{\partial v}{\partial x}\right) = -\nu y \frac{\partial^2 u}{\partial x^2}; \\ \varepsilon_{zx} &= \left(\frac{\partial u}{\partial z} + \frac{\partial w}{\partial x}\right) = -\nu z \frac{\partial^2 u}{\partial x^2} \end{aligned} \quad (3)$$

The stresses induced in the cross section of the bar can be determined, using the three-dimensional Hook's law, as

$$\begin{aligned} \sigma_{xx} &= \frac{E(x)}{(1+\nu)(1-2\nu)} \left((1-\nu)\varepsilon_{xx} + \nu(\varepsilon_{yy} + \varepsilon_{zz}) \right) \\ &= E(x) \frac{\partial u}{\partial x} \\ \sigma_{xy} &= \frac{E(x)}{(1+\nu)(1-2\nu)} \left(\left(\frac{1-2\nu}{2}\right) \varepsilon_{xy} \right) \\ &= -\nu G(x) y \frac{\partial^2 u}{\partial x^2} \end{aligned} \quad (4)$$

$$\begin{aligned}\sigma_{zx} &= \frac{E(x)}{(1+\nu)(1-2\nu)} \left(\left(\frac{1-2\nu}{2} \right) \varepsilon_{zx} \right) \\ &= -\nu G(x) z \frac{\partial^2 u}{\partial x^2} \\ \sigma_{yy} &= \sigma_{zz} = \sigma_{yz} = 0\end{aligned}\quad (4)$$

Now, using Hamilton's principle, the local equation of motion of the nanorod as well as the local boundary conditions can be derived as

$$\frac{\partial N_{xx}}{\partial x} + \nu \frac{\partial^2 (M_{xy} + M_{xz})}{\partial x^2} - \rho(x) A \frac{\partial^2 u}{\partial t^2} + \frac{\partial}{\partial x} \left(\rho(x) \nu^2 I_p \frac{\partial^3 u}{\partial x \partial t^2} \right) = 0 \quad (5)$$

$$\left[\left(N_{xx} + \nu \frac{\partial (M_{xy} + M_{xz})}{\partial x} + \rho(x) \nu^2 I_p \frac{\partial^3 u}{\partial x \partial t^2} \right) \delta u - \nu (M_{xy} + M_{xz}) \delta \left(\frac{\partial u}{\partial x} \right) \right] \Big|_0^L = 0 \quad (6)$$

where

$$N_{xx} = \int \sigma_{xx} dA = E(x) A(x) \frac{\partial u}{\partial x} \quad (7)$$

$$M_{xy} + M_{xz} = \int (y \sigma_{xy} + z \sigma_{xz}) dA = -\nu G(x) I_p \frac{\partial^2 u}{\partial x^2}$$

and $I_p = \int (y^2 + z^2) dA$.

Before converting the local governing equation and boundary conditions to the nonlocal form, it is worth to mention that there are two models of the nonlocal elasticity theory: the differential model and the integral model. Since for a few cases of boundary conditions, e.g., cantilever boundary condition in transverse vibration of nanobeams, the differential model gives a paradox solution, the integral model is proposed (****), "However, the differential model has still some advantages in comparison with the integral model. The differential model makes it possible to obtain the exact solution of a problem with a low computational volume. Furthermore, the differential model is still a prevalent size dependent model for investigation of various mechanical behaviors. It is also worth to mention that however the paradoxes of the differential model are removed by the integral model or other ways, it is not reported that the integral model has a higher accuracy than the differential one. In other words, we cannot definitely express that which one can properly capture the behaviors of nanostructures. Therefore, approve or reject of the differential model requires more studies and investigations. Based on the above descriptions, the authors are used the differential nonlocal elasticity model.

In the nonlocal elasticity theory, the nonlocal parameter is $\mu = (e_0 a)^2$, where e_0 is the small length scale coefficient and a is the internal characteristic length. Based on the nonlocal elasticity of Eringen's theory, the stress tensor on a particular point of a body depends on the strain tensor at all points on that body. Therefore, the nonlocal stress tensor is defined as $(1 - \mu \nabla^2) \sigma^{nl} = \sigma^l$. Therefore, the nonlocal governing equation of motion and the nonlocal boundary

conditions can be obtained by multiplying Eqs. (5) and (6) by $(1 - \mu \nabla^2)$ as follows

$$\frac{\partial (1 - \mu \nabla^2) N_{xx}^{nl}}{\partial x} + \nu \frac{\partial^2 (1 - \mu \nabla^2) (M_{xy}^{nl} + M_{xz}^{nl})}{\partial x^2} - (1 - \mu \nabla^2) \left(\rho(x) A \frac{\partial^2 u}{\partial t^2} \right) + (1 - \mu \nabla^2) \frac{\partial}{\partial x} \left(\rho(x) \nu^2 I_p \frac{\partial^3 u}{\partial x \partial t^2} \right) = 0 \quad (8)$$

$$\left[\left((1 - \mu \nabla^2) N_{xx}^{nl} + \nu \frac{\partial (1 - \mu \nabla^2) (M_{xy}^{nl} + M_{xz}^{nl})}{\partial x} + (1 - \mu \nabla^2) \left(\rho(x) \nu^2 I_p \frac{\partial^3 u}{\partial x \partial t^2} \right) - \nu (1 - \mu \nabla^2) (M_{xy}^{nl} + M_{xz}^{nl}) \delta \left(\frac{\partial u}{\partial x} \right) \right) \delta u \right] \Big|_0^L = 0 \quad (9)$$

where μ is the nonlocal parameter, $\nabla^2 = \partial^2 / \partial x^2$ is the one-dimensional Laplacian operator, and superscript *nl* denotes nonlocal. In addition

$$\begin{aligned}(1 - \mu \nabla^2) N_{xx}^{nl} &= N_{xx} = E(x) A \frac{\partial u}{\partial x} \\ (1 - \mu \nabla^2) (M_{xy}^{nl} + M_{xz}^{nl}) &= M_{xy} + M_{xz} \\ &= -\nu G(x) I_p \frac{\partial^2 u}{\partial x^2}\end{aligned}\quad (10)$$

Substituting Eq. (10) in Eqs. (8) and (9) results in the nonlocal equation of motion and the nonlocal boundary conditions in terms of deflection as follows

$$\begin{aligned}\frac{\partial}{\partial x} \left(E(x) A(x) \frac{\partial u}{\partial x} \right) - \frac{\partial^2}{\partial x^2} \left(\nu^2 G(x) I_p \frac{\partial^2 u}{\partial x^2} \right) - \rho(x) A(x) \frac{\partial^2 u}{\partial t^2} + \mu \frac{\partial^2}{\partial x^2} \left(\rho(x) A(x) \frac{\partial^2 u}{\partial t^2} \right) + \frac{\partial}{\partial x} \left(\rho(x) \nu^2 I_p \frac{\partial^3 u}{\partial x \partial t^2} \right) - \mu \frac{\partial^3}{\partial x^3} \left(\rho(x) \nu^2 I_p \frac{\partial^3 u}{\partial x \partial t^2} \right) = 0\end{aligned}\quad (11)$$

$$\left[\left(E(x) A(x) \frac{\partial u}{\partial x} - \frac{\partial}{\partial x} \left(\nu^2 G(x) I_p \frac{\partial^2 u}{\partial x^2} \right) + \rho(x) \nu^2 I_p \frac{\partial^3 u}{\partial x \partial t^2} - \mu \frac{\partial^2}{\partial x^2} \left(\rho(x) \nu^2 I_p \frac{\partial^3 u}{\partial x \partial t^2} \right) \right) \delta u + \left(\nu^2 G(x) I_p \frac{\partial^2 u}{\partial x^2} \right) \delta \left(\frac{\partial u}{\partial x} \right) \right] \Big|_0^L = 0 \quad (12)$$

The equation of motion of the conventional Bishop rod (Rao 2007) can be obtained from Eq. (11) by setting $\mu = 0$.

3. Free axial vibration analysis

For free axial vibration analysis of AFG nanorods a harmonic relation for the axial displacement is considered

$$u(x, t) = U(x)e^{i\omega t} \tag{13}$$

where ω is the natural axial frequency of AFG nanorod.

Using Eq. (13), Eqs. (11) and (12) can be expressed as

$$\begin{aligned} \frac{d}{dx} \left(E(x)A \frac{dU(x)}{dx} \right) - \frac{d^2}{dx^2} \left(v^2 G(x)I_p \frac{d^2 U(x)}{dx^2} \right) \\ + \rho(x)A\omega^2 U(x) \\ - \mu\omega^2 \frac{d^2}{dx^2} (\rho(x)AU(x)) \\ - \frac{d}{dx} \left(\rho(x)v^2 I_p \omega^2 \frac{dU(x)}{dx} \right) \\ + \mu \frac{d^3}{dx^3} \left(\rho(x)v^2 I_p \omega^2 \frac{dU(x)}{dx} \right) = 0 \end{aligned} \tag{14}$$

$$\begin{aligned} \left[\left(E(x)A \frac{dU(x)}{dx} - \frac{d}{dx} \left(v^2 G(x)I_p \frac{d^2 U(x)}{dx^2} \right) \right. \right. \\ \left. \left. - \rho(x)v^2 I_p \omega^2 \frac{dU(x)}{dx} \right. \right. \\ \left. \left. + \mu \frac{d^2}{dx^2} \left(\rho(x)v^2 I_p \omega^2 \frac{dU(x)}{dx} \right) \right) \delta U(x) \right. \\ \left. + \left(v^2 G(x)I_p \frac{d^2 U(x)}{dx^2} \right) \delta \left(\frac{dU(x)}{dx} \right) \right] \Big|_0^L = 0 \end{aligned} \tag{15}$$

3.1 Solution by harmonic differential quadrature (HDQ) method

To solve the nonlocal governing equation of motion of AFG nanorod, Eq. (14), and accordingly to obtain nonlocal axial frequencies of AFG nanorods, HDQ method is utilized. It is shown that the HDQ method is more efficient than the ordinary differential quadrature (DQ) method for solving the mechanical problems especially vibrational problems (Malekzadeh and Karami 2005, Striz *et al.* 1995, Bert and Malik 1996), “In this method, the partial derivative of a function, with respect to a spatial variable at a given discrete point, approximated by a linear summation of weighted function values at all discrete points chosen in the solution domain of the spatial variable. Suppose the domain of considered AFG nanorod is $(0 < x < L)$ and being discretized by N points along x coordinate. If $F(x)$ representing either of deformation function (u) within the AFG nanorod domain, then the derivatives of $F(x)$ with respect to x at the point x_i can be expressed discretely as

$$\frac{d^n F(x_i)}{dx^n} = \sum_{k=1}^N A_{ik}^{(n)} F(x_k) \quad ; n = 1, \dots, N - 1 \tag{16}$$

where $A_{ik}^{(n)}$ is the weighting coefficient in conjunction to the n -th order derivative of $F(x)$, at the discrete points x_i . The description of HDQ method and how to choose the positions of the nodal points using Chebyshev polynomials were presented by Civalek (2004), “Now, the HDQM can be used to discretize the Eq. (14), governing equation, and Eq. (15), boundary condition equation. Before do this, $X = x/L$ and $\bar{U} = U/L$ are used to obtain the non-dimensional form of Eqs. (14) and (15) as follows

$$\begin{aligned} \frac{1}{L} \frac{d}{dX} \left(E(X)A \frac{d\bar{U}(X)}{dX} \right) - \frac{1}{L^3} \frac{d^2}{dX^2} \left(v^2 G(X)I_p \frac{d^2 \bar{U}(X)}{dX^2} \right) \\ + \rho(X)A\omega^2 L\bar{U}(X) \\ - \frac{\mu\omega^2}{L} \frac{d^2}{dX^2} (\rho(X)A\bar{U}(X)) \\ - \frac{1}{L} \frac{d}{dX} \left(\rho(X)v^2 I_p \omega^2 \frac{d\bar{U}(X)}{dX} \right) \\ + \frac{\mu}{L^3} \frac{d^3}{dX^3} \left(\rho(X)v^2 I_p \omega^2 \frac{d\bar{U}(X)}{dX} \right) = 0 \end{aligned} \tag{17}$$

$$\begin{aligned} \left[\left(E(X)A \frac{d\bar{U}(X)}{dX} - \frac{1}{L^2} \frac{d}{dX} \left(v^2 G(X)I_p \frac{d^2 \bar{U}(X)}{dX^2} \right) \right. \right. \\ \left. \left. - \rho(X)v^2 I_p \omega^2 \frac{d\bar{U}(X)}{dX} \right. \right. \\ \left. \left. + \frac{\mu}{L^2} \frac{d^2}{dX^2} \left(\rho(X)v^2 I_p \omega^2 \frac{d\bar{U}(X)}{dX} \right) \right) \delta L\bar{U}(X) \right. \\ \left. + \left(\frac{v^2 G(X)I_p}{L} \frac{d^2 \bar{U}(X)}{dX^2} \right) \delta \left(\frac{d\bar{U}(X)}{dX} \right) \right] \Big|_0^1 = 0 \end{aligned} \tag{18}$$

Now by implementing HDQM, the discretized forms of governing equation and boundary condition equation at $X_i = x_i/L$ are obtained as

$$\begin{aligned} \frac{1}{L} \sum_{k=1}^N \left(A(i, k)E(X_k)A \sum_{j=1}^N (A(k, j)\bar{U}(X_j)) \right) \\ - \frac{1}{L^3} \sum_{k=1}^N \left(B(i, k)v^2 G(X_k)I_p \sum_{j=1}^N (B(k, j)\bar{U}(X_j)) \right) \\ + \rho(X_i)A\omega^2 L\bar{U}(X_i) - \frac{\mu\omega^2}{L} \sum_{k=1}^N (B(i, k)\rho(X_k)A\bar{U}(X_k)) \end{aligned} \tag{19}$$

$$\begin{aligned} - \frac{1}{L} \sum_{k=1}^N \left(A(i, k)\rho(X_k)v^2 I_p \omega^2 \sum_{j=1}^N (A(k, j)\bar{U}(X_j)) \right) \\ + \frac{\mu}{L^3} \sum_{k=1}^N \left(C(i, k)\rho(X_k)v^2 I_p \omega^2 \sum_{j=1}^N (A(k, j)\bar{U}(X_j)) \right) \\ = 0 \end{aligned}$$

$$\begin{aligned} \left[\left(E(X_i)A \sum_{k=1}^N (A(i, k)\bar{U}(X_k)) \right. \right. \\ \left. \left. - \frac{1}{L^2} \sum_{k=1}^N \left(A(i, k)v^2 G(X_k)I_p \sum_{j=1}^N (B(k, j)\bar{U}(X_j)) \right) \right) \right] \end{aligned} \tag{20}$$

$$\begin{aligned}
& -\rho(X_i)v^2I_p\omega^2\sum_{k=1}^N(A(i,k)\bar{U}(X_k)) \\
& +\frac{\mu}{L^2}\sum_{k=1}^N\left(B(i,k)\rho(X_k)v^2I_p\omega^2\sum_{j=1}^N(A(k,j)\bar{U}(X_j))\right) \\
& \delta L\bar{U}(X_i)+\left(\frac{v^2G(X_i)I_p}{L}\sum_{k=1}^N(B(i,k)\bar{U}(X_k))\right) \\
& \delta\left(\sum_{k=1}^N(A(i,k)\bar{U}(X_k))\right)\Bigg|_0^1=0
\end{aligned} \quad (20)$$

Applying the discretized forms of boundary conditions, Eq. (20), into the discretized forms of governing equation, Eq. (19), and separating domain and boundary degrees of freedom (DOF), the following assembled matrix equations are obtained

$$\begin{bmatrix} [K_{bb}] & [K_{bd}] \\ [K_{db}] & [K_{dd}] \end{bmatrix} \begin{Bmatrix} \{\bar{U}_b\} \\ \{\bar{U}_d\} \end{Bmatrix} = \omega^2 \begin{bmatrix} [0] & [0] \\ [M_{db}] & [M_{dd}] \end{bmatrix} \begin{Bmatrix} \{0\} \\ \{\bar{U}_d\} \end{Bmatrix} \quad (21)$$

where $\{\bar{U}_b\}$ and $\{\bar{U}_d\}$ represent the boundary and domain DOF, respectively, as

$$\begin{aligned}
\{\bar{U}_b\} &= \{\bar{U}(X_1), \bar{U}(X_2), \bar{U}(X_{N-1}), \bar{U}(X_N)\}; \\
\{\bar{U}_d\} &= \{\bar{U}(X_2), \bar{U}(X_3), \dots, \bar{U}(X_{N-3}), \bar{U}(X_{N-2})\}
\end{aligned} \quad (22)$$

After doing some mathematical simplifications on Eq. (21), the natural frequencies of the AFG nanorod can be calculated by solving the following relation

$$\begin{aligned}
& [[M_{dd}] - [M_{db}][K_{bb}]^{-1}[K_{bd}]]^{-1}[[K_{dd}] \\
& \quad - [K_{db}][K_{bb}]^{-1}[K_{bd}]]\{\bar{U}_d\} \\
& = \omega^2\{\bar{U}_d\}
\end{aligned} \quad (23)$$

Based on the above outlined formulations and by aids of the MATHEMATICA program solver a self-developed computer program is written by which the natural frequencies of the AFG nanorod can be obtained.

4. Results and discussion

Eq. (23) gives natural frequencies of AFG nanorods with clamped-clamped boundary condition. This section is divided into two parts. At first, the results of present study are compared with literature for homogeneous nanorods modeled based on the Bishop's theory to show the reliability and accuracy of the present formulation and results. Next, benchmark results including natural frequencies are presented with considering effects of the nonlocal parameter, the shear stiffness and inertia of lateral motions, the nanorod dimensions, the frequency number, and the value of gradient index. In the following, effect of the inertia of the lateral motions and the shear stiffness is called the theory effect, for the brevity.

4.1 Comparison study

As mentioned in Introduction section, references

Table 1 Natural frequencies of CC nanorod ($E = 70$ GPa, $\rho = 2370$ kg.m⁻³, $L = 20$ nm, $R = 0.5$ nm)

Mode number	μ (nm ²)	Present (NBT****)	Rao (2007) (LBT***)	Kiani (2010) (NST**)	Şimşek (2012) (AFG-NST*)
1		135.856	135.856	135.868	135.868
2	0	271.643	271.642	271.735	271.735
3		407.292	407.290	407.603	407.603
1		134.210	-	134.220	134.220
2	1	259.155	-	259.241	259.241
3		368.432	-	368.710	368.710
1		129.610	-	129.618	129.618
2	4	230.008	-	230.083	230.083
3		296.396	-	296.620	296.620

* Axially functionally graded- Nonlocal Simple theory;

** Nonlocal simple theory;

*** Local Bishop's theory;

**** Nonlocal Bishop's theory

considering the small scale effects on free longitudinal vibration of nanorods implemented the simple theory (Aydogdu 2009, Goushegir and Faroughi 2016) or the Rayleigh theory (Nazemnezhad and Kamali 2016) for modeling of nanorods. This causes that in **Table 1** the nonlocal results of the present work are compared with those given by Kiani (2010) and Şimşek (2012). The exact solution (Kiani 2010) and Galerkin method (Şimşek 2012) are utilized to obtain free vibration frequencies. The local natural frequencies presented by Rao (2007) and calculated by the exact solution of Bishop's model are also listed in Table 1. Table 1 shows that the results of the present study which are obtained by the HDQM are very close to those obtained by the exact solution of Bishop's model. Furthermore, Table 1 exhibits that the results of nonlocal Bishop's model are a little smaller than those obtained based on the Simple theory. This is due to this fact that the Bishop's theory considers the inertia of the lateral motions and the shear stiffness effects while this is not the case in the Simple theory. It can be concluded from Table 1 that the present formulation and results are reliable and accurate.

4.2 Benchmark results

In this section, to consider the effects of the small scale, the inertia of the lateral motions and the shear stiffness on the free longitudinal vibration of nanorods, four types of frequency ratios are defined as Eq. (24).

Table 2 Material properties of AFG nanorod

Material property	Unit	Left side of nanorod	Right side of nanorod
Young's modulus (E)	GPa	70	210
Shear modulus (G)	GPa	27	85
Density (ρ)	kg.m ⁻³	2700	2370
Poisson's ratio (ν)	-	0.3	0.3

The numerical values of FR_1 , FR_2 , FR_3 , and FR_4 represent the small scale effect on natural frequencies of thin AFG nanorods, the theory effect on natural frequencies of thin AFG nanorods, the small scale and the theory effects on natural frequencies of thin AFG nanorods, and the small scale effect on natural frequencies of thick AFG nanorods, respectively.

$$FR_1 = \frac{NLST}{LST} \equiv \frac{\text{Nonlocal frequency based on the simple theory}}{\text{Local frequency based on the simple theory}}$$

$$FR_2 = \frac{LBT}{LST} \equiv \frac{\text{Local frequency based on the Bishop's theory}}{\text{Local frequency based on the simple theory}}$$

$$FR_3 = \frac{NLBT}{LST} \equiv \frac{\text{Nonlocal frequency based on the Bishop's theory}}{\text{Local frequency based on the simple theory}}$$

$$FR_4 = \frac{NLBT}{LBT} \equiv \frac{\text{Nonlocal frequency based on the Bishop's theory}}{\text{Local frequency based on the Bishop's theory}}$$
(24)

In the following, an AFG nanorod with circular cross-section and clamped-clamped boundary condition is investigated. The material properties of AFG nanorod are selected as Table 2.

At first, effects of the length of the AFG nanorod on the frequency ratios are investigated. To this end, variations of the first, third and fifth frequency ratios (FR_3 and FR_4) of AFG nanorod are plotted in Fig. 2 for three different values of gradient index ($m = 0, 1, 10$), “The diameter and nonlocal parameter of AFG nanorod are assumed to be 3 nm and 0.5 nm^2 , respectively. Fig. 2 displays that for all mode numbers and all values of the gradient index, all frequency ratio curves are located below the horizontal line representing $FR = 1$. This shows the decreasing effects of the small scale and the theory parameters on natural axial frequencies of AFG nanorods. In addition, by increasing

the length of AFG nanorod frequency ratios increase and approach their horizontal asymptotes, $FR = 1$.

This implies that increasing the length of the AFG nanorod decreases both the small scale and theory effects. The other point from Fig. 2 is that for all values of the gradient index by increasing the frequency number, values of FR_3 and FR_4 decrease and the difference between FR_3 and FR_4 curves increases. Decreasing of values of frequency ratios indicates that the decreasing effects of the small scale and theory parameters increase at higher frequency numbers. Besides, increasing the difference between FR_3 and FR_4 curves means the theory effect on axial frequencies of AFG nanorods becomes more at higher frequency numbers. The last interesting point from Fig. 2 is that the reducing effects of the small scale and theory parameters vary with a change in the value of the gradient index. Fig. 2 exhibits that increasing the gradient index value from zero to one increases the reducing effects of the small scale and theory parameters while changing the gradient index value from one to ten causes a reduction in the reducing effects of the small scale and theory parameters. The dependency of frequency ratios on the gradient index value concluded from Fig. 2 causes that variations of the frequency ratios versus the gradient index value to be considered in details in the following.

Fig. 3 displays variations of frequency ratios versus the value of the gradient index for various frequency numbers. Fig. 3 confirms the results presented in Fig. 2 regarding dependency of frequency ratios on the value of the gradient index. It is seen from Fig. 3 that the dependency of the frequency ratios on the gradient index becomes more at higher frequency numbers. If the frequency ratios do not depend on the gradient index, the small scale and theory effects on a desired natural frequency is the same for all values of the gradient index. This point is interesting because in literature (Nazemnezhad and Hosseini-Hashemi 2014) it is reported that linear frequency ratios of functionally graded nanobeams are independent of the gradient index in transverse vibration. It is better to state that frequency ratios of nanobeams which are functionally graded in the thickness direction only in the case of nonlinear transverse vibration depend on the gradient index.

In order to survey about the effects of the second geometrical parameter, i.e., the diameter of AFG nanorod,

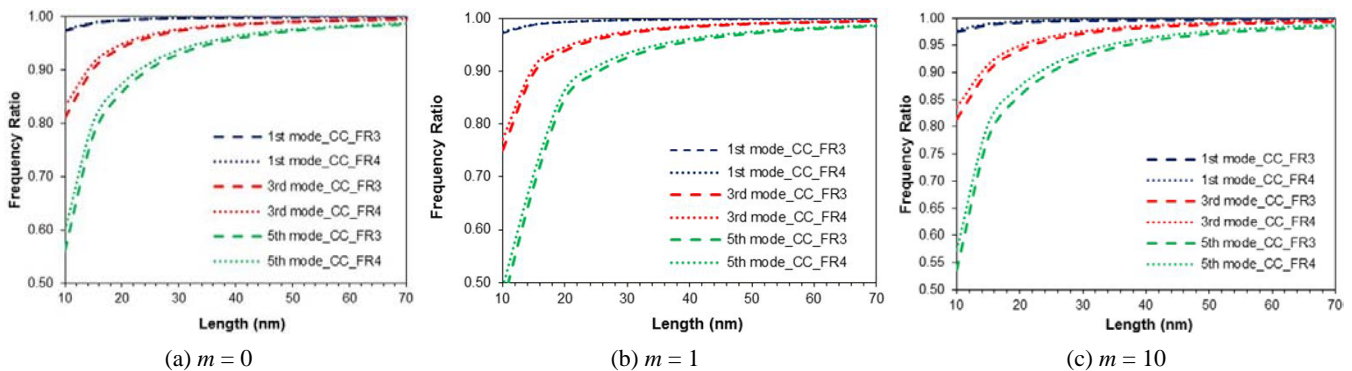


Fig. 2 Variations of FR_3 and FR_4 versus the length for the first, third and fifth natural frequencies, $D = 3 \text{ nm}$, $\mu = 0.5 \text{ nm}^2$ and (a) $m = 0$; (b) $m = 1$; (c) $m = 10$

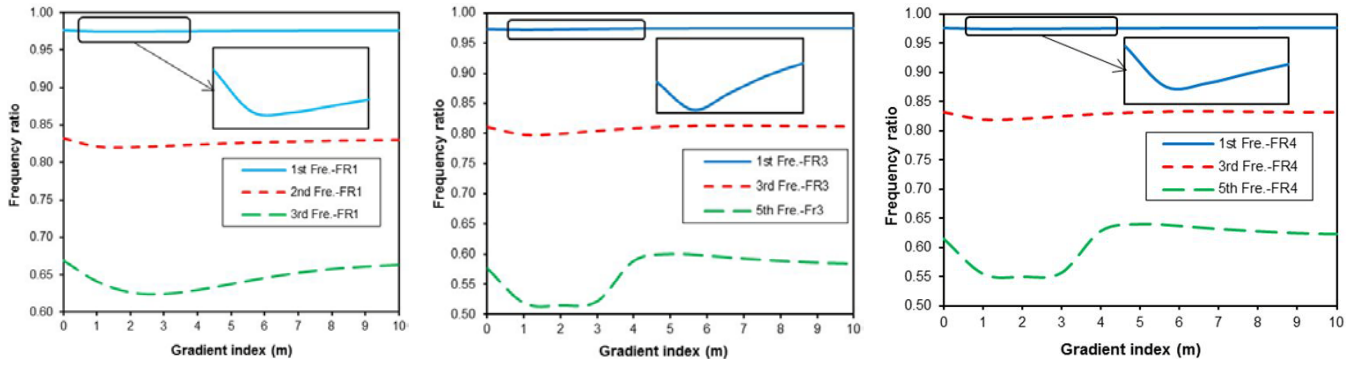


Fig. 3 Variations of frequency ratios versus the value of the gradient index for various frequency numbers, $L = 20 \text{ nm}$, $R = 5 \text{ nm}$, $\mu = 0.5 \text{ nm}^2$

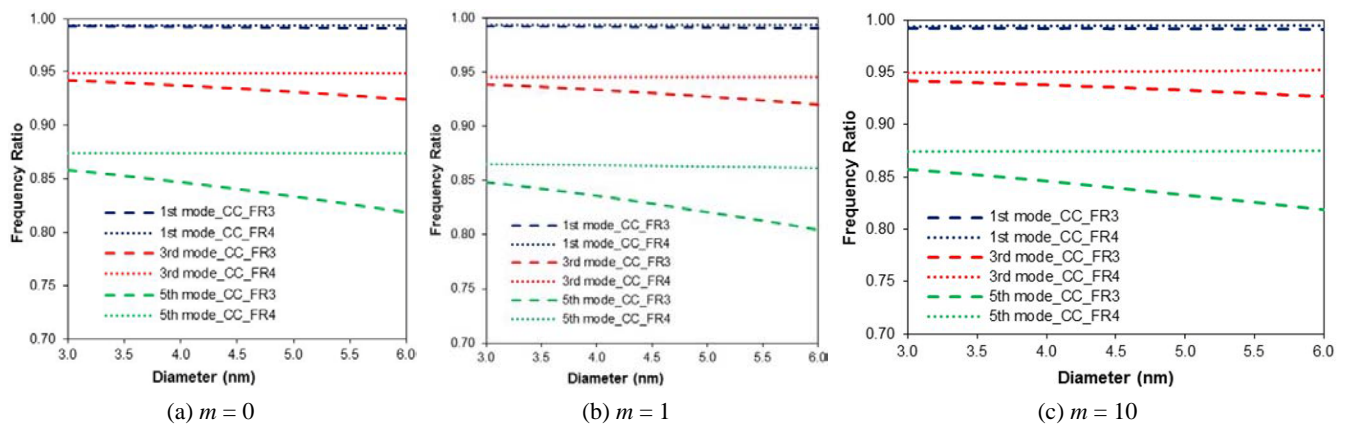


Fig. 4 Variations of FR_3 and FR_4 versus the diameter for the first, third and fifth natural frequencies, $L = 20 \text{ nm}$, $\mu = 0.5 \text{ nm}^2$ and (a) $m = 0$; (b) $m = 1$; (c) $m = 10$

on natural frequencies, in Fig. 4 variations of FR_3 and FR_4 versus the diameter of AFG nanorod are plotted. The first interesting point of Fig. 4 is that the effect of the small scale parameter on the axial natural frequencies is independent of

the diameter of the AFG nanorod while it is the other way round for the effect of the theory parameter. Fig. 4 shows that by increasing the diameter of the AFG nanorod the effect of the theory parameter increases and this increase is

Table 3 Fundamental nonlocal axial frequencies of AFG nanorod based on the simple and Bishop theories and frequency ratios for various values of the length of AFG nanorod ($D = 3 \text{ nm}$ and $\mu = 0.5 \text{ nm}^2$)

L (nm)	$m = 0$						$m = 10$					
	NLST (GHz)	NLBT (GHz)	FR1	FR2	FR3	FR4	NLST (GHz)	NLBT (GHz)	FR1	FR2	FR3	FR4
10	248.529	247.775	0.97620	0.99697	0.97324	0.97620	447.579	447.108	0.97591	0.99630	0.97489	0.97851
15	167.894	167.666	0.98921	0.99865	0.98787	0.98921	302.412	301.868	0.98908	0.99757	0.98730	0.98970
20	126.516	126.419	0.99389	0.99924	0.99313	0.99388	227.895	227.471	0.99382	0.99793	0.99197	0.99402
25	101.435	101.386	0.99608	0.99951	0.99559	0.99608	182.722	182.382	0.99603	0.99806	0.99418	0.99611
30	84.631	84.602	0.99727	0.99966	0.99693	0.99727	152.453	152.169	0.99724	0.99810	0.99538	0.99727
35	72.593	72.575	0.99799	0.99975	0.99774	0.99799	130.770	130.525	0.99797	0.99811	0.99610	0.99799
40	63.549	63.537	0.99846	0.99985	0.99827	0.99842	114.478	114.262	0.99845	0.99812	0.99656	0.99845
45	56.506	56.498	0.99878	0.99985	0.99863	0.99878	101.791	101.598	0.99876	0.99810	0.99687	0.99877
50	50.8673	50.8611	0.99901	0.99988	0.99889	0.99901	91.634	91.4588	0.99900	0.99809	0.99710	0.99900
55	46.2510	46.2463	0.99919	0.99990	0.99909	0.99916	83.318	83.1577	0.99918	0.99808	0.99726	0.99918
60	42.4022	42.3986	0.99931	0.99991	0.99923	0.99932	76.385	76.237	0.99931	0.99807	0.99738	0.99931

Table 4 Fundamental nonlocal axial frequencies of AFG nanorod based on the simple and Bishop theories and frequency ratios for various values of the diameter of AFG nanorod ($L = 20 \text{ nm}$ and $\mu = 0.5 \text{ nm}^2$)

D (nm)	$m = 0$						$m = 10$					
	NST (GHz)	NBT (GHz)	FR1	FR2	FR3	FR4	NST (GHz)	NBT (GHz)	FR1	FR2	FR3	FR4
3.00	126.516	126.419	0.9939	0.99924	0.99313	0.9939	227.895	227.471	0.9938	0.99851	0.99197	0.99345
3.25	126.516	126.402	0.9939	0.99911	0.99299	0.9939	227.895	227.463	0.9938	0.99786	0.99193	0.99406
3.50	126.516	126.384	0.9939	0.99897	0.99285	0.9939	227.895	227.452	0.9938	0.99778	0.99188	0.99410
3.75	126.516	126.365	0.9939	0.99881	0.99270	0.9939	227.895	227.532	0.9938	0.99768	0.99183	0.99413
4.00	126.516	126.344	0.9939	0.99864	0.99254	0.9939	227.895	227.424	0.9938	0.99758	0.99176	0.99417
4.25	126.516	126.322	0.9939	0.99847	0.99237	0.9939	227.895	227.493	0.9938	0.99745	0.99169	0.99422
4.50	126.516	126.299	0.9939	0.99829	0.99219	0.9939	227.895	227.386	0.9938	0.99732	0.99160	0.99426
4.75	126.516	126.274	0.9939	0.99809	0.99200	0.9939	227.895	227.444	0.9938	0.99718	0.99150	0.99430
5.00	126.516	126.248	0.9939	0.99789	0.99178	0.9939	227.895	227.339	0.9938	0.99703	0.99139	0.99434
5.25	126.516	126.221	0.9939	0.99767	0.99157	0.9939	227.895	227.385	0.9938	0.99687	0.99127	0.99439
5.50	126.516	126.193	0.9939	0.99745	0.99135	0.9939	227.895	227.283	0.9938	0.99669	0.99115	0.99444

more at higher frequency numbers. It is also seen from Fig. 4 that at higher frequency numbers the effect of the small scale parameter increases. The conclusions of Fig. 4 are reliable for all values of the gradient index.

In order to present numerical data for future researches, Tables 3-4 are prepared. In Tables 3-4 the fundamental nonlocal axial frequencies based on the simple and bishop theories and values of FR_1 , FR_2 , FR_3 , and FR_4 are listed for various values of the length and the diameter of AFG nanorod, respectively. From Tables 3-4 obtaining the value of a desired axial natural frequency is possible. It can be seen from Tables 3-4 that for $m = 0$ values of the FR_1 and FR_4 are the same. This means that the effect of the small scale parameter on the axial natural frequencies of AFG nanorods is independent of the rod theory. This is not the case for the effect of the small scale parameter on the axial natural frequencies of AFG nanorods when the value of the gradient index is greater than zero.

In the final part of the research, it is tried to find out the appropriate values of the small scale parameter in such a way that its effect becomes equal to the effect of the theory parameter. To this end, values of the FR_2 (implying the effect of the theory parameter) are compared with those of FR_4 (implying the effect of the small scale parameter) for various values of the small scale parameters. The computations for the fundamental frequency ratios are shown in Fig. 5. It is seen from Fig. 5 that for certain values of the small scale parameter, the FR_2 and FR_4 curves intersect, indicating that for these values reducing influence of the small scale parameter on the natural axial frequencies of the AFG nanorod becomes equal to the reducing effect of the theory parameter. It can also be stated that for the small scale parameter with values less than these certain values, the reducing influence of the theory parameter is dominant and for values of the small scale parameter larger than the values of the intersection point, the decreasing effect of the small scale parameter becomes dominant.

In order to provide more comprehensive results for the values of the small scale parameter at intersection points of

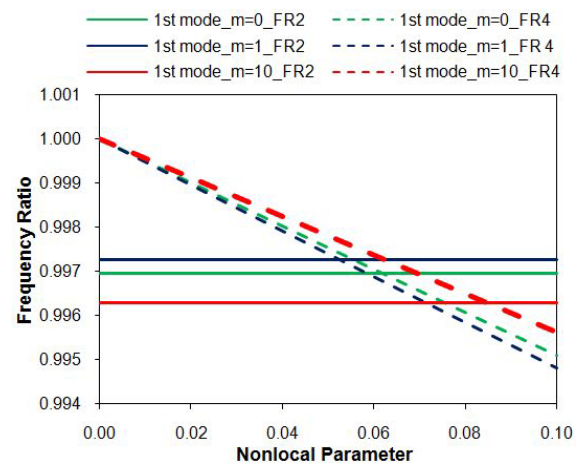


Fig. 5 Variations of the fundamental FR_2 and FR_4 versus the small scale parameter ($L = 10 \text{ nm}$ and $D = 3 \text{ nm}$)

FR_2 and FR_4 curves, Table 5 is prepared. Table 5 gives some interesting points as:

- (a) For a certain frequency number, the desired small scale parameter increases by increasing the length of the AFG nanorod. This implies that by increasing the length of the AFG nanorod the effect of the small scale parameter on natural axial frequencies decreases more than the effect of the theory parameter. Therefore a larger small scale parameter is required. This is more considerable for AFG nanorods with higher gradient index number.
- (b) For a certain length of the AFG nanorod, a smaller value for the desired small scale parameter is required at higher frequency numbers. This means that at higher frequency numbers the effect of the small scale parameter on natural axial frequencies increases more than the effect of the theory parameter. Therefore a smaller nonlocal parameter

Table 3 The values of the small scale parameter in which its effect becomes equal to the effect of the theory parameter, equality of FR_2 and FR_4 ($D = 3$ nm)

Frequency number	L (nm)	μ (nm ²)		
		$m = 0$	$m = 1$	$m = 10$
1	10	0.061	0.048	0.087
	15	0.065	0.050	0.134
	20	0.069	0.054	0.2108
	25	0.070	0.056	0.301
2	10	0.060	0.058	0.0706
	15	0.061	0.059	0.0814
	20	0.0615	0.0595	0.099
	25	0.062	0.06	0.121
3	10	0.06	0.058	0.0655
	15	0.061	0.061	0.0706
	20	0.062	0.0615	0.0784
	25	0.063	0.062	0.088
4	10	0.0585	0.0571	0.0627
	15	0.0604	0.06	0.0665
	20	0.061	0.061	0.0709
	25	0.062	0.0615	0.0771
5	10	0.0566	0.0545	0.0597
	15	0.0596	0.0587	0.0638
	20	0.0606	0.06	0.0673
	25	0.061	0.061	0.071

is required. This is also more considerable for AFG nanorods with higher gradient index number likes the conclusion of part *a*.

It is worth to note here that the importance of the data listed in Table 5 is that there is not reported any value for the small scale parameter in the free axial vibration of the AFG nanorods. Therefore the data of Table 5 can be useful for implementing the appropriate theory of rods for modelling of the axial vibration of AFG nanorods. This is possible when the experiment results of the axial natural frequencies of the AFG nanorods are available.

5. Conclusions

In this paper, free axial vibration of AFG nanorods is studied by focusing on the inertia of lateral motions, shear stiffness and nonlocal parameter effects. To this end, nonlocal Bishop's theory is used. The following conclusions could be highlighted from this study:

- Influence of the small scale and theory parameters depends on the value of the gradient index.
- The effect of the small scale parameter on the axial natural frequencies is independent of the diameter of the AFG nanorod while it is the other way round for the effect of the theory parameter.

- The effect of the small scale parameter on the axial natural frequencies of homogenous nanorods is independent of the rod theory while this is not the case for the effect of the small scale parameter on the axial natural frequencies of AFG nanorods when the value of the gradient index is greater than zero.
- It is possible to obtain certain values for the small scale parameter in such a way that its effect becomes equal to the effect of the theory parameter. For a certain frequency number these values increase by increasing the length of the AFG nanorod, and for a certain length of the AFG nanorod a smaller value for the small scale parameter is required at higher frequency numbers.
- Each of two factors, the small scale and the theory, can have a dominant influence on the axial frequencies of the AFG nanorods relative to the other. This depends on the value of the small scale parameter, dimensions of the AFG nanorod, the frequency number, and the value of the gradient index.

Acknowledgments

The financial support of national elite foundation of Islamic Republic of Iran with the grant number 15/83734 is acknowledged.

The authors also would like to deeply appreciate the research council of Damghan University for its cooperation.

References

- Adhikari, S., Murmu, T. and McCarthy, M.A. (2013), "Dynamic finite element analysis of axially vibrating nonlocal rods", *Finite Elem. Anal. Des.*, **63**, 42-50.
- Adhikari, S., Murmu, T. and McCarthy, M.A. (2014), "Frequency domain analysis of nonlocal rods embedded in an elastic medium", *Physica E: Low-dimen. Syst. Nanostruct.*, **59**, 33-40.
- Akgöz, B. and Civalek, Ö. (2011), "Buckling analysis of cantilever carbon nanotubes using the strain gradient elasticity and modified couple stress theories", *J. Computat. Theor. Nanosci.*, **8**, 1821-1827.
- Akgöz, B. and Civalek, Ö. (2013), "Longitudinal vibration analysis of strain gradient bars made of functionally graded materials (FGM)", *Compos. Part B: Eng.*, **55**, 263-268.
- Akgöz, B. and Civalek, Ö. (2017), "Effects of thermal and shear deformation on vibration response of functionally graded thick composite microbeams", *Compos. Part B: Eng.*, **129**, 77-87.
- Allahkarami, F., Nikkrah-Bahrami, M. and Saryazdi, M.G. (2017), "Damping and vibration analysis of viscoelastic curved microbeam reinforced with FG-CNTs resting on viscoelastic medium using strain gradient theory and DQM", *Steel Compos. Struct., Int. J.*, **25**(2), 141-155.
- Amar, L.H.H., Kaci, A., Yeghnem, R. and Tounsi, A. (2018), "A new four-unknown refined theory based on modified couple stress theory for size-dependent bending and vibration analysis of functionally graded micro-plate", *Steel Compos. Struct., Int. J.*, **26**(1), 89-102.
- Assadi, A. and Farshi, B. (2011), "Size-dependent longitudinal and transverse wave propagation in embedded nanotubes with consideration of surface effects", *Acta Mech.*, **222**(1-2), 27-39.

- Aydogdu, M. (2009), "Axial vibration of the nanorods with the nonlocal continuum rod model", *Physica E: Low-dimen. Syst. Nanostruct.*, **41**(5), 861-864.
- Aydogdu, M. (2014), "A nonlocal rod model for axial vibration of double-walled carbon nanotubes including axial Van der Waals force effects", *J. Vib. Control*, **21**(16), 3132-3154.
- Belkorissat, I., Houari, M.S.A., Tounsi, A., Bedia, E.A. and Mahmoud, S.R. (2015), "On vibration properties of functionally graded nano-plate using a new nonlocal refined four variable mode", *Steel Compos. Struct., Int. J.*, **18**(4), 1063-1081.
- Bert, C.W. and Malik, M. (1996), "Differential quadrature method in computational mechanics: a review", *Appl. Mech. Rev.*, **49**(1), 1-28.
- Bounouara, F., Benrahou, K.H., Belkorissat, I. and Tounsi, A. (2016), "A nonlocal zeroth-order shear deformation theory for free vibration of functionally graded nanoscale plates resting on elastic foundation", *Steel Compos. Struct., Int. J.*, **20**(2), 227-249.
- Civalek, Ö. (2004), "Application of differential quadrature (DQ) and harmonic differential quadrature (HDQ) for buckling analysis of thin isotropic plates and elastic columns", *Eng. Struct.*, **26**(2), 171-186.
- Faroughi, S. and Shaat, M. (2017), "Poisson ratio effects on the mechanics of auxetic nanobeams", *Eur. J. Mech. / A Solids*, **70**, 8-14.
- Faroughi, S., Goushegir, S.M.H., Khodaparast, H.H. and Friswell, M.I. (2017), "Nonlocal elasticity in plates using novel trial functions", *Int. J. Mech. Sci.*, **130**, 221-233.
- Fernández-Sáez, J., Zaera, R., Loya, J. and Reddy, J. (2016), "Bending of Euler-Bernoulli beams using Eringen's integral formulation: a paradox resolved", *Int. J. Eng. Sci.*, **99**, 107-116.
- Goushegir, S.M.H. and Faroughi, S. (2016), "Analysis of axial vibration of non-uniform nanorods using boundary characteristic orthogonal polynomials", *Modares Mech. Eng.*, **16**(1), 203-212.
- Goushegir, S.M.H. and Faroughi, S. (2017), "Free vibration and wave propagation of thick plates using the generalized nonlocal strain gradient theory", *J. Theor. Appl. Vib. Acoust.*, **3**(2), 165-198.
- Güven, U. (2014), "Love-Bishop rod solution based on strain gradient elasticity theory", *Comptes Rendus Mecanique*, **342**, 8-16.
- Hsu, J.-C., Lee, H.-L. and Chang, W.-J. (2011), "Longitudinal vibration of cracked nanobeams using nonlocal elasticity theory", *Current Appl. Phys.*, **11**(6), 1384-1388.
- Karličić, D., Cajić, M., Murmu, T. and Adhikari, S. (2015), "Nonlocal longitudinal vibration of viscoelastic coupled double-nanorod systems", *Eur. J. Mech.-A/Solids*, **49**, 183-196.
- Kiani, K. (2010), "Free longitudinal vibration of tapered nanowires in the context of nonlocal continuum theory via a perturbation technique", *Physica E: Low-dimen. Syst. Nanostruct.*, **43**(1), 387-397.
- Li, X.F., Shen, Z.B., and Lee, K.Y. (2017), "Axial wave propagation and vibration of nonlocal nanorods with radial deformation and inertia", *ZAMM-Journal of Applied Mathematics and Mechanics/Zeitschrift für Angewandte Mathematik und Mechanik*, **97**, 602-616.
- Malekzadeh, P. and Karami, G. (2005), "Polynomial and harmonic differential quadrature methods for free vibration of variable thickness thick skew plates", *Eng. Struct.*, **27**(10), 1563-1574.
- Murmu, T. and Adhikari, S. (2010), "Nonlocal effects in the longitudinal vibration of double-nanorod systems", *Physica E: Low-dimen. Syst. Nanostruct.*, **43**(1), 415-422.
- Narendar, S. and Gopalakrishnan, S. (2011), "Axial wave propagation in coupled nanorod system with nonlocal small scale effects", *Compos. Part B: Eng.*, **42**(7), 2013-2023.
- Nazemnezhad, R. and Hosseini-Hashemi, S. (2014), "Nonlocal nonlinear free vibration of functionally graded nanobeams", *Compos. Struct.*, **110**, 192-199.
- Nazemnezhad, R. and Kamali, K. (2016), "Investigation of the inertia of the lateral motions effect on free axial vibration of nanorods using nonlocal Rayleigh theory", *Modares Mech. Eng.*, **16**(5), 19-28. [In Persian]
- Nguyen, N.-T., Kim, N.-I. and Lee, J. (2014), "Analytical solutions for bending of transversely or axially FG nonlocal beams", *Steel Compos. Struct., Int. J.*, **17**(5), 641-665.
- Rahmani, O., Refaieejad, V. and Hosseini, S. (2017), "Assessment of various nonlocal higher order theories for the bending and buckling behavior of functionally graded nanobeams", *Steel Compos. Struct., Int. J.*, **23**(3), 339-350.
- Rao, S.S. (2007), *Vibration of Continuous Systems*, John Wiley & Sons.
- Romano, G., Barretta, R., Diaco, M. and de Sciarra, F.M. (2017), "Constitutive boundary conditions and paradoxes in nonlocal elastic nanobeams", *Int. J. Mech. Sci.*, **121**, 151-156.
- Shaat, M. and Faroughi, S. (2018), "Influence of surface integrity on vibration characteristics of microbeams", *Eur. J. Mech. - A/Solids*, **71**, 365-377.
- Şimşek, M. (2011), "Forced vibration of an embedded single-walled carbon nanotube traversed by a moving load using nonlocal Timoshenko beam theory", *Steel Compos. Struct., Int. J.*, **11**(1), 59-76.
- Şimşek, M. (2012), "Nonlocal effects in the free longitudinal vibration of axially functionally graded tapered nanorods", *Computat. Mater. Sci.*, **61**, 257-265.
- Striz, A., Wang, X. and Bert, C. (1995), "Harmonic differential quadrature method and applications to analysis of structural components", *Acta Mech.*, **111**(1-2), 85-94.

CC